# SMALL SCALE DISCHARGE STUDIES

J.H. Jacob, J.A. Mangano and M. Rokni
Avco Everett Research Laboratory, Inc.
2385 Revere Beach Parkway
Everett MA 02149



Semi--Annual Report for Period 1 March 1976 to 31 August 1976





Sponsored by

DEFENSE ADVANCED RESEARCH PROJECTS AGENCY
DARPA Order No. 1806

Monitored by

OFFICE OF NAVAL RESEARCH
DEPARTMENT OF THE NAVY
Arlington VA 22217

# SMALL SCALE DISCHARGE STUDIES



J.H. Jacob, J.A. Mangano and M. Rokni
Avco Everett Research Laboratory, Inc.
2385 Revere Beach Parkway
Everett MA 02149



Semi–Annual Report for Period 1 March 1976 to 31 August 1976





Sponsored by

DEFENSE ADVANCED RESEARCH PROJECTS AGENCY
DARPA Order No. 1806

Monitored by

OFFICE OF NAVAL RESEARCH
DEPARTMENT OF THE NAVY
Arlington VA 22217

UNCLASSIFIED

SECURITY CLASSIFICATION OF THIS PAGE (When Data Entered)

| REPORT DOCUMENTATION PAGE | READ INSTRUCTIONS BEFORE COMPLETING FORM |
|---|---|
| 1. REPORT NUMBER | 2. GOVT ACCESSION NO. 3. RECIPIENT'S CATALOG NUMBER |
| 4. TITLE (and Subtitle) (6) SMALL SCALE DISCHARGE STUDIES | 5. TYPE OF REPORT & PERIOD COVERED (9) Semi-Annual Report 1 March [illegible] - 31 Aug 1976 |
| | 6. PERFORMING ORG. REPORT NUMBER |
| 7. AUTHOR(s) (10) J. H. Jacob, J. A. Mangano and M. Rokni | 8. CONTRACT OR GRANT NUMBER(s) (15) N00014-75-C-0662, DARPA Order-1806 |
| 9. PERFORMING ORGANIZATION NAME AND ADDRESS Avco Everett Research Laboratory, Inc. 2385 Revere Beach Parkway Everett, MA 02149 | 10. PROGRAM ELEMENT, PROJECT, TASK AREA & WORK UNIT NUMBERS |
| 11. CONTROLLING OFFICE NAME AND ADDRESS Defense Advanced Research Project Agency DARPA Order No. 1806 | 12. REPORT DATE (11) 31 Aug 76 13. NUMBER OF PAGES 45 |
| 14. MONITORING AGENCY NAME & ADDRESS (if different from Controlling Office) Office of Naval Research Department of the Navy Arlington, VA 22217 (12) 43p. | 15. SECURITY CLASS. (of this report) Unclassified 15a. DECLASSIFICATION/DOWNGRADING SCHEDULE |

16. DISTRIBUTION STATEMENT (of this Report)

Approved for Public Release; Distribution Unlimited.

17. DISTRIBUTION STATEMENT (of the abstract entered in Block 20, if different from Report)

18. SUPPLEMENTARY NOTES

19. KEY WORDS (Continue on reverse side if necessary and identify by block number)
Visible/UV Lasers
Rare Gas Fluoride Lasers
XeF* Laser
XeF* Kinetics

.0004 cub.cm/sec

20. ABSTRACT (Continue on reverse side if necessary and identify by block number)

This report discusses the discharge physics and the formation and quenching processes in typical XeF laser mixtures. We have determined that the discharge physics is dominated by electron impact excitation and ionization of the rare gas metastables. The ionization of the metastables impacts the discharge stability directly while their excitation strongly affects the efficiency of producing XeF*. From our discharge experiments we have determined that Xe (6p) states react with $NF_3$ to produce XeF* with a branching ratio of 0.7. The rate constant for this reaction is $4 \times 10^{-10}$ $cm^3/sec$. The formation and

DD FORM 1 JAN 73 1473 EDITION OF 1 NOV 65 IS OBSOLETE

UNCLASSIFIED

SECURITY CLASSIFICATION OF THIS PAGE (When Data Entered)

Ø4845Ø

quenching processes have been determined by analyzing the dependence of ($B^2\Sigma^+_{1/2} \rightarrow X^2\Sigma^+_{1/2}$) radiation on the partial pressures of Ar, Xe, and $F_2$. In the experiments the XeF* was produced by a high energy e-beam. We have determined the two and three body quenching rates by Ar to be $8 \pm 4 \times 10^{-13}$ $cm^3/sec$ and $1.5 \pm 0.5 \times 10^{-32}$ $cm^6/sec$. Xe quenches XeF* with a three body rate of $3 \pm 1.5 \times 10^{-31}$ $cm^6/sec$; the third body was mainly argon.

B 2 Signa(+) 1/2 goes to X 2 Signa(+) 1/2

4 X 10 to the -13th

cc/sec

X 10 to the -32nd.

cm to the 6th/sec

D to the -31st

## REPORT SUMMARY

In this report we report on the investigations of e-beam controlled discharge of the $XeF^*$ laser discharge. As in the case of $KrF^*$ we find that electron impact excitation and ionization of the rare gas metastables play a dominant role in the discharge physics. We have also thoroughly investigated the formation and quenching kinetics of $XeF^*$ in e-beam pumped laser mixtures. From our data we conclude that both $Xe^+$ and $Xe_2^+$ recombine with $F^-$ to form $XeF^*$. The two and three body quenching rate constants of $XeF^*$ by Ar and Xe have also been measured.

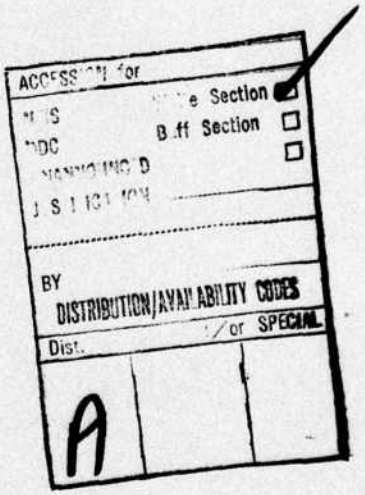

blank

TABLE OF CONTENTS

blank

## LIST OF ILLUSTRATIONS

blank

# I. DISCHARGE MODELING OF THE $XeF^*$ LASER

## A. INTRODUCTION

Laser action in $XeF^*$ was first achieved at AERL by pure e-beam pumping.[1] Subsequently Burnham et al.[2] at NRL and Sutton et al.[3] at Aerospace obtained laser action by UV preionization, avalanche discharge pumping. More recently we have obtained 40 mJ of laser energy in an e-beam ionized, avalanche discharge.[4] We have also investigated in detail the discharge physics of the XeF laser containing ~ 99.5% Ar, 0.4% Xe and 0.1 - 0.2% $NF_3$.

The physics of rare gas/halogen discharges is dominated by the excited species when the fractional population of the rare gas metastables exceeds $10^{-9}$.[5] For example, an important process in XeF laser discharges is the excitation of low lying metastables to higher lying states. This process can strongly influence the secondary electron energy distribution and therefore the efficiency of producing the metastables (which react with $NF_3$ to form $XeF^*$ -- the upper laser level). The dominant ionization mechanism in XeF laser discharges is ionization of the xenon and argon metastables, i.e., two-step ionization. For this discharge, metastable ionization rates of 1-5 x $10^7$ $sec^{-1}$ are typical so that this process strongly

---

(1) C.A. Brau and J.J. Ewing, Appl. Phys. Lett. 27, 435 (1975).

(2) R. Burnham, D. Harris and N. Djeu, Appl. Phys. Lett. 28, 86 (1976).

(3) D.C. Sutton, S.N. Suchard, O.L. Gibb and C.P. Wange, Appl. Phys. Lett. 28, 522 (1976).

(4) J.A. Mangano, J.H. Jacob and J.B. Dodge, Appl. Phys. Lett., October 1, 1976.

(5) J.H. Jacob and J.A. Mangano, Appl. Phys. Lett. 28, 724 (1976).

influences discharge stability. These important excited state processes will be described in more detail subsequently.

B. SIMPLIFIED XeF KINETICS

In this section the dominant kinetics of the XeF laser discharge will be discussed. The high energy electrons $\vec{e}$ ionize the mixture forming mainly argon ions

$$\vec{e} + Ar \rightarrow Ar^+ + \vec{e} + e_s \quad (1)$$

The secondarly electrons $e_s$ are rapidly lost by attachment to $NF_3$ to form the negative halogen ion

$$e_s + NF_3 \rightarrow NF_2 + F^- \quad (2)$$

The secondary electrons gain energy in the applied electric field and most of the discharge energy initially goes into producing argon metastable $Ar^*$

$$e_s + Ar \rightarrow Ar^* + e_s \quad (3)$$

There are three principal reactions by which the argon metastables are lost

$$Ar^* + Xe \rightarrow Xe^{**} + Ar \quad (4)$$

$$Ar^* + 2Ar \rightarrow Ar_2^* + Ar \quad (5)$$

$$Ar^* + NF_3 \rightarrow ArF^* + NF_2 \quad (6)$$

The rate constant for reaction (4) has been measured to be $1.8 \times 10^{-10}$ and $3 \times 10^{-10}$ $cm^3/sec$ for Ar ($^3P_2$) and ar ($^3P_0$) respectively.[6] Reaction (5) has a three-body rate constant of $1.7 \times 10^{-32}$ $cm^6/sec$ for Ar ($^3P_1$), $0.9 \times 10^{-32}$ $cm^6/sec$ for Ar ($^1P_1$) and $1.6 \times 10^{-32}$ $cm^6/sec$ for Ar ($^3P_2$).[7]

---

(6) L.G. Piper, J.E. Velazco and D.W. Setser, J. Chem. Phys. 59, 3323 (1973).

(7) M. Bourene, O. Dutnuit and J. LeCalve, J. Chem. Phys. 63, 1668 (1975).

Assuming a gas kinetic mixing rate of these states by electrons, the loss rates of $Ar^*$ by reactions (4) and (5) will be only marginally affected. So we will assume a mean rate of $2 \times 10^{-10}$ $cm^3/sec$ for reaction (4) and $10^{-32}$ $cm^3/sec$ for reaction (5). The argon metastables react with $NF_3$ to form $ArF^*$ with a rate constant of $1.4 \times 10^{-10}$ $cm^3/sec$.[8] The branching ratio for this reaction is yet to be determined. Extrapolating from reactions of $Xe^*$ and $Kr^*$ with $NF_3$[7] one might conclude that reaction (6) has a branching ratio of about 0.5. At a mixture pressure of four atmospheres with 0.4% Xe and 0.1% $NF_3$, the rates for reactions (4), (5) and (6) are $8 \times 10^7$, $2.5 \times 10^7$ and $1.4 \times 10^7$ $sec^{-1}$. So about 15% of the $Ar^*$ is channeled into $ArF^*$. Most of the energy in $ArF^*$ will produce $XeF^*$ by the following reaction

$$ArF^* + Xe \rightarrow XeF^* + Ar \qquad (7)$$

The remainder of the energy is presumably radiated on the $ArF^*$ bands. As reaction (7) proceeds with a rate constant $\sim 10^{-9}$ $cm^3/sec$, 75% of the $ArF^*$ is to be channeled into $XeF^*$.

The argon excimers $Ar_2^*$ will be deactivated at least as rapidly by Xe to form highly excited xenon states $Xe^{**}$. This means that 70-80% of the $Ar_2^*$ will end up as $Xe^{**}$. The remainder of the $Ar_2^*$ will be radiated. So we can conclude that the argon metastables transfer their energy to the xenon metastables with a 75% efficiency. The $Xe^{**}$ thus formed will react with the $NF_3$ to form $XeF^*$. The branching ratio and rate constant for this reaction are not known. However, from our discharge data we have inferred a reaction rate constant of $4 \times 10^{-10}$ $cm^3/sec$ and a branching ratio of 0.7.

---

(8) J.E. Velazco, J.H. Kolts and D.W. Setser J. Chem. Phys. 65, 3468 (1976).

There are, of course, inefficiencies that arise from discharge pumping. The most severe are the electron impact excitation of the argon and xenon metastables

$$e_s + Ar^* \rightarrow Ar^{**} + e_s \quad (8)$$

$$e_s + Xe^* \rightarrow Xe^{**} + e_s \quad (9)$$

The rare gas metastables are similar to the alkalis and probably have large impact cross section to higher lying levels. Figure 1 shows the expected cross section for $Xe^*$ (Cs). Also shown in Figure 1 are the cross sections for the excitation of ground state Xe and Ar and the ionization of $Xe^*$ (Cs).

C. DISCHARGE PHYSICS

As we have stated earlier, the physics of the discharge is strongly affected by the electron impact excitation and ionization of the rare gas metastables. To model these effects, we have treated the xenon metastables as cesium and the argon metastables as potassium, an analogy used successfully in predicting the emission spectra of rare-gas monohalides.

Some of the electron-impact cross sections used in our model are shown in Figure 1. The cross section for excitation from the 6s configuration to the 6p configuration in Cs ($Xe^*$) has a peak value of 90 $Å^2$ at 8 eV. The peak value of the metastable-excitation is 40 times the peak value of the argon excitation cross section. More important, however, is the ability of most of the electrons to excite the 6s-6p transitions -- which have a threshold of 1.5 eV -- but only the high energy tail of the electron energy distribution can produce metastables from the ground state.

In Figures 2, 3 and 4 we show the predictions of the Boltzmann code. Figure 2 shows the percentage of energy that goes into producing

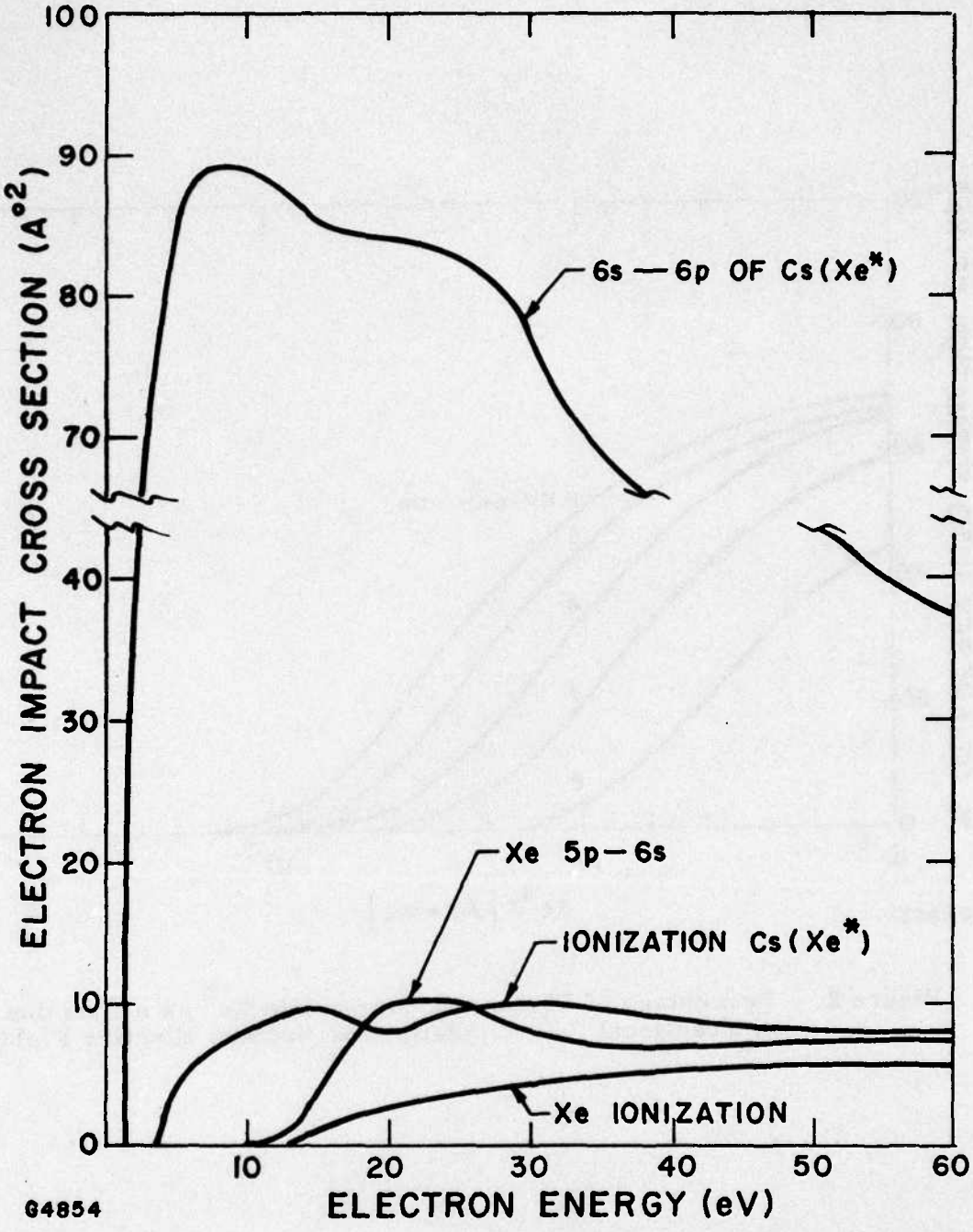


Figure 1 Electron-Impact Cross Sections of Cesium ($Xe^*$) and Xenon as Functions of Electron Energy

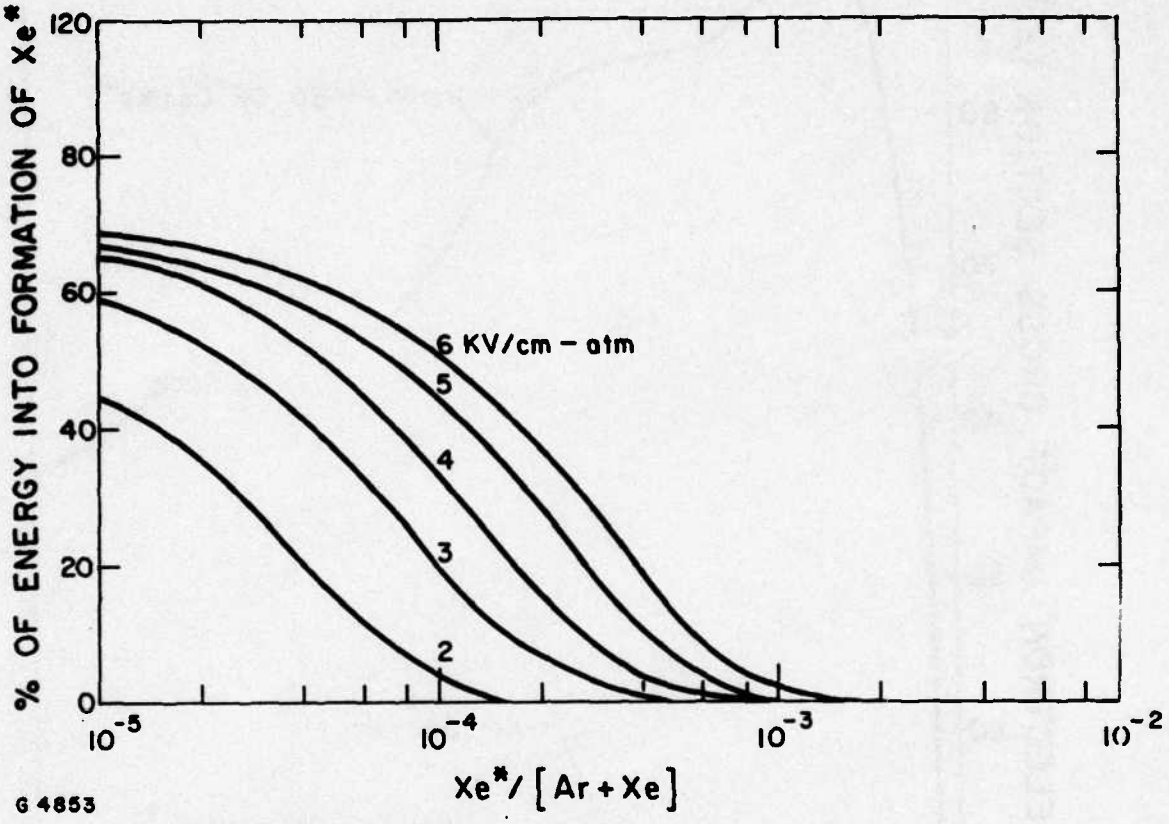


Figure 2 Percentage of Discharge Energy into $Xe^*$ as a Function of Fractional $Xe^*$ Population for Various Electric Fields

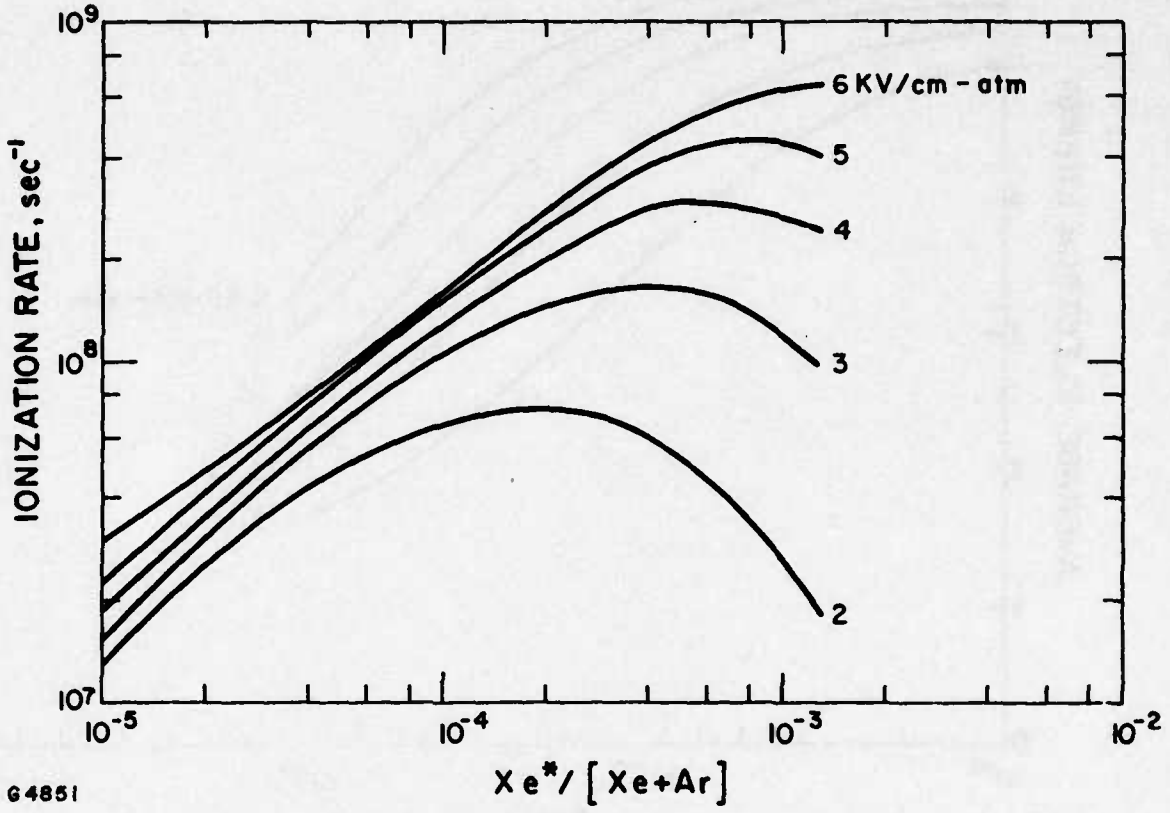


Figure 3 Ionization Rate as a Function of Fractional $Xe^*$ Population

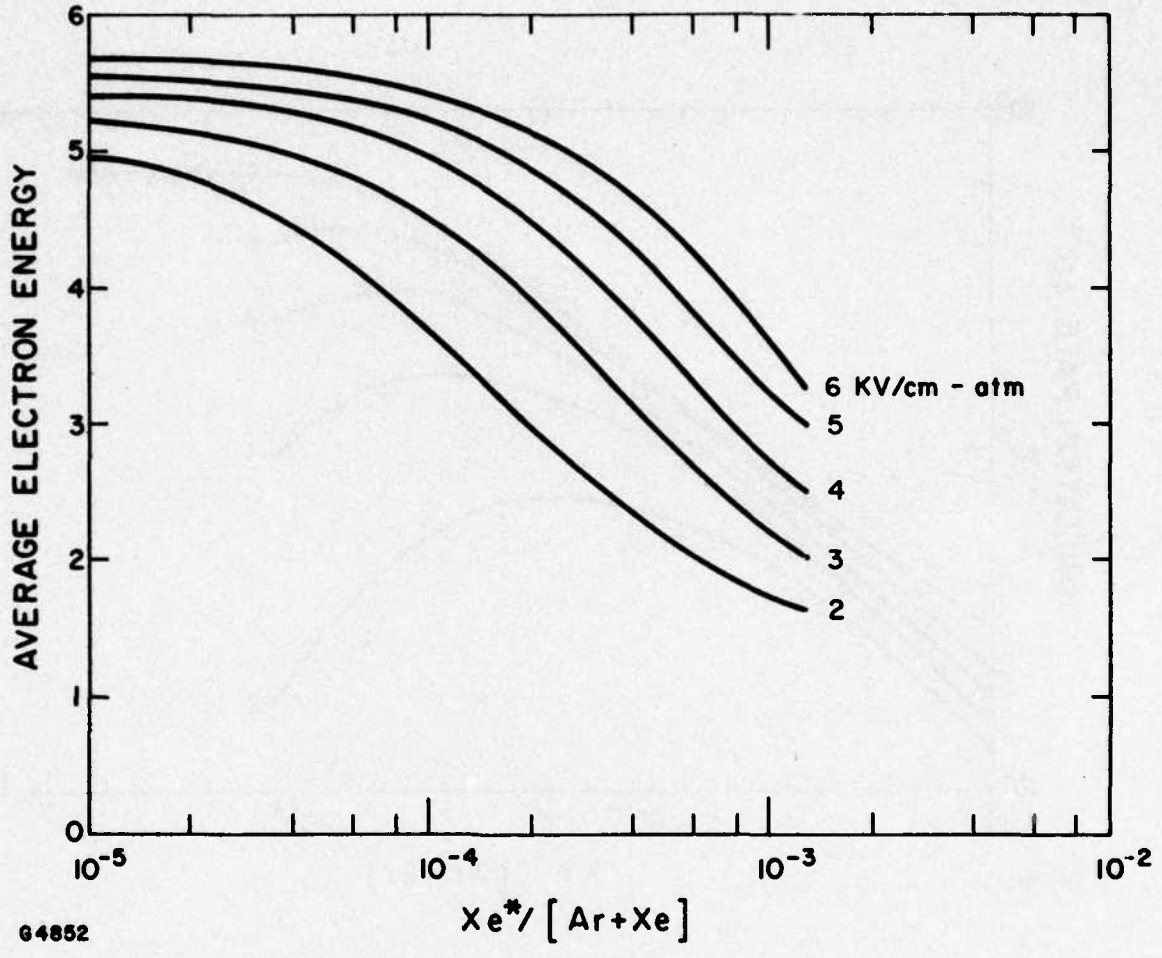


**Figure 4** Average Electron Energy as a Function of Fractional $Xe^*$ Population

$Xe^*$ as a function of the fractional metastable population $Xe^*/(Kr + Ar)$ for electric fields of 2-6 kV/cm atm. It is apparent from Figure 2 that the efficiency of producing the metastables is a strong function of the $Xe^*$ population. For example, the efficiency of forming $Xe^*$ is almost 45% when the fractional population is $10^{-5}$ and the electric field is 2 kV/cm atm. This efficiency decreases to less than 10% when the fractional population is increased to $10^{-4}$. The decrease in efficiency can be made up by increasing the electric field. Figure 3 shows the ionization rate as a function of the fractional metastable population. Figure 4 is a plot of the average electron energy as a function of the fractional metastable population. Notice that the electrons cool as the metastable population increases. The cooling effect is much stronger at smaller electric fields.

Using the rate constants predicted by the Boltzmann code, we have developed a self-consistent kinetics code that follows the temporal evolution of the secondary electrons, positive and negative ions, $Ar^*$, $Ar_2$, $Xe^{**}$ and $XeF^*$. We couple our kinetics code to a simultaneous set of differential equations that describe the electrical circuit. The outputs of this code include the temporal evolution of the discharge current and voltage and the $XeF^*$ fluorescence for a given preionization level, capacitor charge voltage and gas mixture.

The predictions of this discharge model have been compared with our $XeF^*$ laser discharge experiments. The top trace in Figure 5 is the e-beam current in the discharge cavity. The lower trace is the fluorescence as observed by a photomultiplier after the signal passes through a 1/4 meter Jarrel Ash monochromator tuned to 3520 Å. The cavity was filled with a 1 atm mix of 99.4% Ar, 0.4% Xe and 0.2% $NF_3$. The dashed

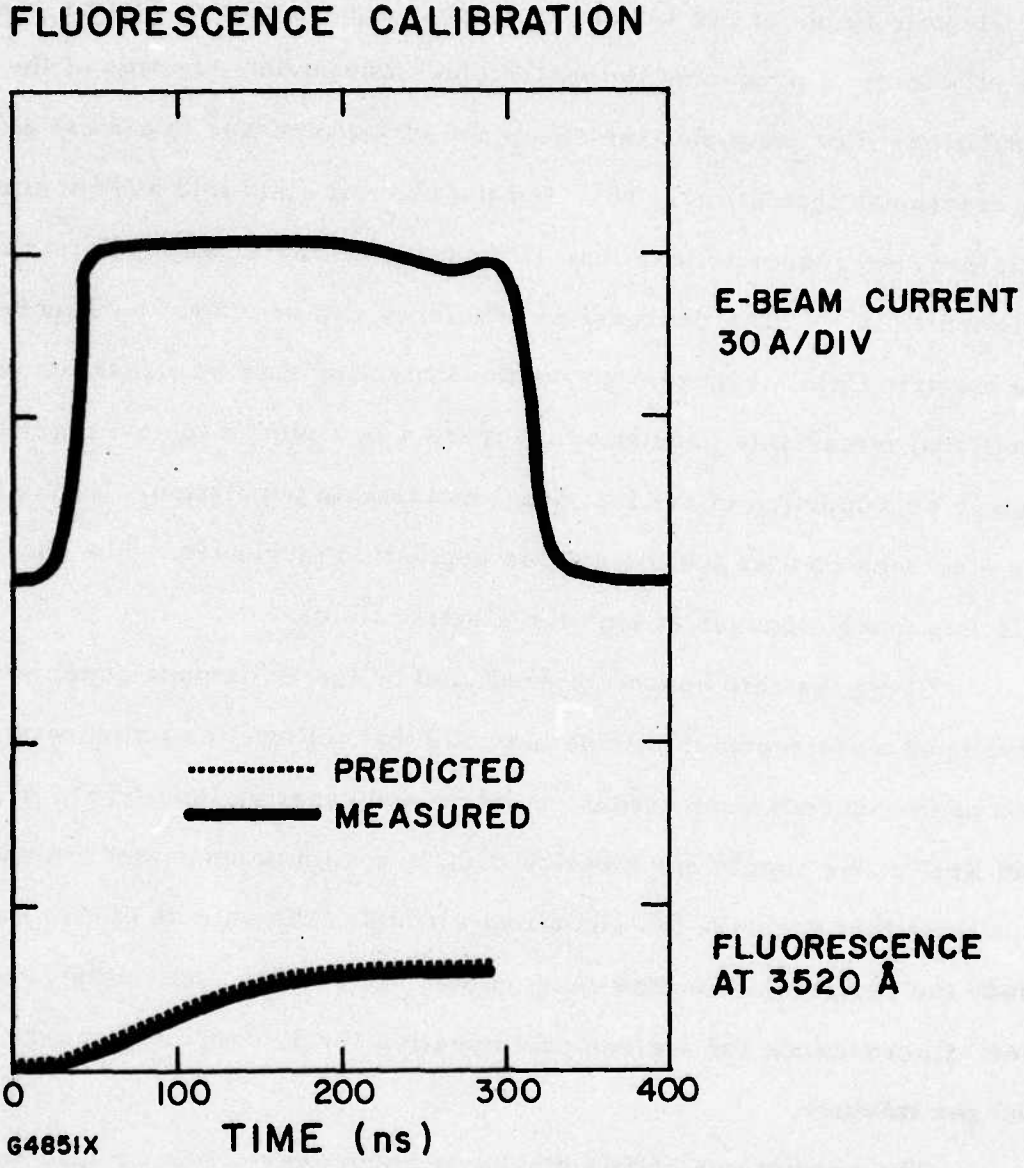


Figure 5 Measured and Predicted Fluorescence for Pure E-Beam Pumping. The discharge cavity contained 99.4% Ar, 0.4% Xe and 0.2% $NF_3$.

trace is the prediction of the code. The amplitude of this predicted trace is adjusted to closely match the measured fluorescence. This amplitude normalization was necessary as we did not have an absolute calibration on the fluorescence emanating from the discharge. For subsequent comparisons between experiment and theory no further adjustments were made.

Once the $XeF^*$ fluorescence amplitude was normalized, we measured the magnitude and efficiency of discharge produced $XeF^*$ fluorescence enhancement. Figure 6 shows the experimental results and theoretical predictions when the 0.3 $\mu$F capacitor is charged to 8 kV. The top trace is the discharge voltage. The second trace is the discharge current. The third trace is the $XeF^*$ fluorescence. By the end of the pulse the enhancement in the fluorescence is 2.5. The metastables are being produced with the same efficiency as by pure e-beam pumping. Note that the predicted fluorescence is 30% higher than the measured fluorescence. The reduced measured fluorescence can be explained if the branching ratio from $Xe^{**}$ (see reaction (4)) is 0.7. Further, to predict the current in the discharge we have used a rate constant for reaction (4) of $4 \times 10^{-10}$ $cm^3/sec$. If a slower rate constant is used the predicted discharge current does not reach a steady state value.

## D. CONCLUSIONS

In conclusion, our discharge model predicts that rare gas metastables can be produced with high efficiency (60%) as long as the fractional metastable population is kept sufficiently small ($< 2\text{-}3 \times 10^{-5}$). We have also inferred that $Xe^{**}$ reacts with $NF_3$ to produce $XeF^*$ with a branching ratio of 0.7. The rate constant for this reaction is $4 \times 10^{-10}$ $cm^3/sec$.

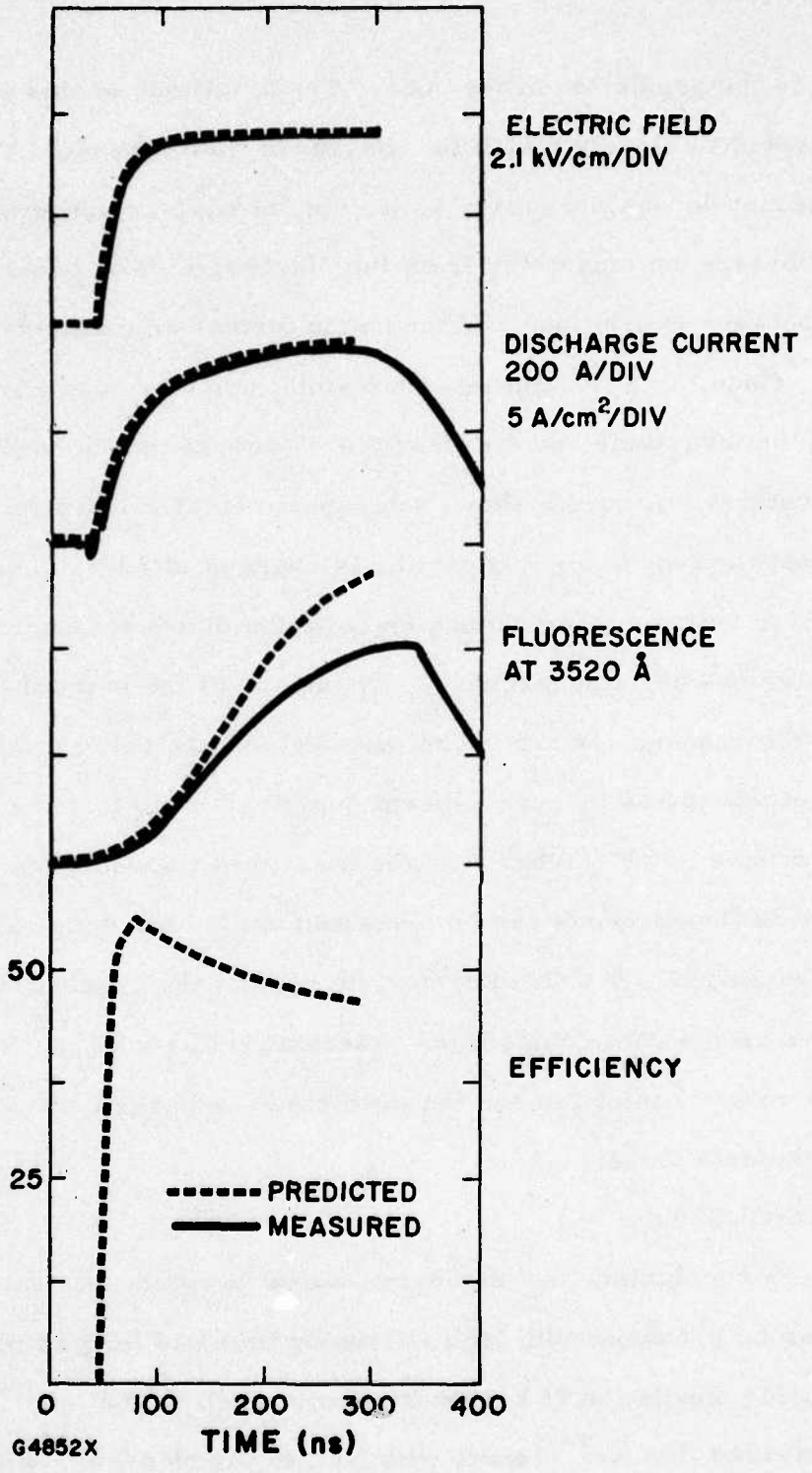


Figure 6 Measured and Predicted Fluorescence When Capacitor is Charged to 8 kV

## II. FORMATION AND QUENCHING OF $XeF^*$

### A. INTRODUCTION

Efficient scaling of the $XeF^*$ laser[1-5] to high average power requires knowledge of the processes responsible for the formation and quenching of the upper laser level. From the formation kinetics one can determine the upper state production efficiency. The quenching kinetics enables one to choose the appropriate mix and determine the laser saturation flux.[9] For efficient laser power extraction the cavity flux should be much greater than the saturation flux. In this section we report on measurements of the quenching rates of $XeF^*$ by Ar and Xe. These rates were obtained by analyzing the dependence of $XeF^*$ fluorescence intensity on the partial pressures of Ar, Xe and $F_2$. We have determined the rate constants for the following processes:

$$XeF^* + Ar \rightarrow 8 \pm 4 \times 10^{-13} \text{ cm}^3/\text{sec}$$

$$XeF^* + Ar + M \rightarrow 1.5 \pm 0.5 \times 10^{-32} \text{ cm}^6/\text{sec}$$

$$XeF^* + Xe + M \rightarrow 3 \pm 1.5 \times 10^{-31} \text{ cm}^6/\text{sec}$$

The third body M was mainly argon.

### B. EXPERIMENTAL APPARATUS

Argon, xenon and fluorine were premixed and excited by a high energy e-beam. The resulting $XeF^*$ fluorescence amplitude was measured by a photodiode via a 5 nm bandpass filter centered at 352 nm. To ensure that the emission was representative of the overall kinetic processes, we repeated the experiments with a 50 nm bandpass filter. This changed the

---

(9) W.W. Rigrod, J. Appl. Phys. 36, 2487 (1965).

amplitude of the photodiode signal by a constant factor over the whole pressure range of interest. Hence we concluded that the attenuation of $XeF^*$ ($B^2\Sigma^+_{1/2} \rightarrow X^2\Sigma^+_{1/2}$) radiation observed through the 5 nm bandpass filter was constant when the mixture pressure was varied. The mixtures used contained mainly Ar, 7.6 torr $F_2$, and varing amounts of Xe (from 7.6 torr to 150 torr). For a given run however we kept the xenon concentration fixed and increased the argon partial pressure from 0.5 atmospheres up to 4 atmospheres because at lower pressures the spectra changed radically.[8] This change is possibly due to the lack of collisional relaxation of the manifold of upper states at low gas pressures.

Research grade (Matheson) Ar and Xe were used without any further purification. The gases were analyzed by Gollob Analytical Service, Inc., and found to have less than 100 ppm of $O_2$, $N_2$, $H_2O$ and $CO_2$ impurities. The $F_2$ was 98% pure. The electron gun apparatus used in these experiments has been described previously.[4] This device produces an electron beam with an energy of 150 keV and a current density of 0.2 - 5 $A/cm^2$ for 300 nsec. The cross sectional dimensions of the e-beam were 2 cm x 22 cm. The beam interacted with the mixture in a teflon cell 0.5 cm deep in the beam direction; this short dimension insured a linear increase in the energy deposition with pressure for pressures up to 4 atmospheres.

C. ANALYSIS OF DATA

Table 1 lists the dominant formation kinetics. The high energy electrons deposit their energy into $F_2$, Xe and Ar in a ratio roughly proportional to their mass densities. One important question in analyzing the experimental data is to decide the major kinetic pathways of the positive ions $Ar^+$ and $Xe^+$. Reaction (12) gives a formation rate for $ArF^*$ that is proportional to

TABLE 1. DOMINANT FORMATION REACTIONS

$$e + \begin{matrix} Ar \\ He \end{matrix} + \rightarrow \begin{matrix} Ar^+ \\ Xe^+ \end{matrix} + \vec{e} + e_s \quad (10)$$

$$e_s + F_2 + \rightarrow F + F^- \quad (11)$$

$$Ar^+ + F^- + M \rightarrow ArF^* + M \quad (12)$$

$$Ar^+ + Ar + M \rightarrow Ar_2^+ + M \quad (13)$$

$$Ar_2^+ + F^- \rightarrow ArF^* + Ar \quad (14)$$

$$ArF^* + Xe \rightarrow XeF^* + Ar \quad (15)$$

$$Xe^+ + F^- + M \rightarrow XeF^* + M \quad (16)$$

$$Xe^+ + Xe + M \rightarrow Xe_2^+ + M \quad (17)$$

$$Xe_2^+ + F^- + \rightarrow XeF^* + Xe \quad (18)$$

$[F^-]\ [Ar^+]$. Since $[F^-] \sim [Ar^+] \sim \sqrt{I_{eb}}$ ($I_{eb}$ = e-beam current) one expects that $ArF^*$ formation and hence $XeF^*$ (via reaction (15) by this path to be proportional to $I_{eb}$. Similarly reaction (16) gives a production rate of $XeF^*$ linearly proportional to $I_{eb}$. The data showed $XeF^*$ fluorescence to vary linearly with e-beam current from 0.2 A/cm$^2$ to 5 A/cm$^2$ for the full range of mixtures and pressures used, which is thus consistent with the foregoing discussion. It is also known, however, that reaction (13) and (17) are significant sinks for $Ar^+$ and $Xe^+$, especially at the higher pressures. Only by hypothesizing reactions (14) and (18) can we maintain a total mechanism of ion chemistry which leaves $XeF^*$, and hence its fluorescence, linearly proportional to $I_{eb}$. Thus alternate species such as $Ar_2F^*$ and $Xe_2F^*$ cannot be major products of reactions (14) and (18).[10]

Once $XeF^*$ is formed, it can radiate (with spontaneous lifetime of 16 nsec)[11] or be quenched by $F_2$, Xe or Ar. Recently Brashears, Setser and DesMarteau[12] have measured the quenching rate constants of $XeF^*$ by $F_2$ and Xe and found them to be $3.3 \times 10^{-10}$ cm$^3$/sec and $2.9 \times 10^{-11}$ cm$^3$/sec respectively. All processes involved reach a steady state on a time scale much less than the 300 nsec e-beam pulse. So the photodiode signal can be written as

---

(10) A. Hawryluk, J.A. Mangano and J.H. Jacob, 3rd Summer Colloquium on Electronic Transition Lasers, Sept. 7-10 (1976). D.C. Lorents, R.M. Hill, D.L. Huestis, M.V. McCusker and N.H. Nakano, ibid.

(11) G.J. Eden and S.K. Searles, 3rd Summer Colloquium on Electronic Transition Lasers, Sept. 7-10 (1976).

(12) H.C. Brashears, Jr., D.W. Setser and D. DesMarteau (unpublished). These experiments were performed by photodissociating $XeF_2$ in a cell capable of going to one atmosphere.

$$S = \frac{\alpha + \alpha_{Ar} P_{Ar}}{\gamma + \xi_{F_2} P_{F_2} + \xi_{Xe} P_{Xe} + \xi_{Ar} P_{Ar} + \delta_{Xe} P_{Xe} P + \delta_{Ar} P_{Ar} P} \quad (19)$$

where $P_{F_2}$, $P_{Ar}$ and $P_{Xe}$ are the pressures of $F_2$, Ar and Xe respectively. P is the total pressure, $\alpha_{Ar}$ is proportional to the efficiency of generation of $XeF^*$ from the e-beam energy deposited in the Ar. $\alpha$ is the contribution to the $XeF^*$ formation from the e-beam energy deposited in Xe. Both $\alpha$ and $\alpha_{Ar}$ are constants for constant $P_{Xe}$ and $P_{Ar}$. $\gamma$ is the inverse spontaneous lifetime. $\xi_{F_2}$, etc., are the two body quenching rate constants of $F_2$ etc. $\delta_{Xe}$ and $\delta_{Ar}$ are the three body quenching rate constants by argon and xenon. We have ignored the three body quenching by $F_2$ because of the low fluorine concentrations used. For example, a three-body rate constant of $10^{-30}$ $cm^6/sec$ would lower the measured two body rate constant by Ar by 20%. It is very difficult to obtain this rate constant because of the rapid quenching of $XeF^*$ by $F_2$.[12]

For each experimental run the signal intensity was measured as a function of $P_{Ar}$ keeping $P_{F_2}$ and $P_{Xe}$ constant. (A run consists of a series of experimental data for various values of $P_{Ar}$.) Seven different runs were made for $P_{Xe}$ = 7.6 up to 152 torr. For each run the data so obtained was fitted to a polynomial

$$S = \sum_n A_n P_{Ar}^n \quad (20)$$

In Eq. (20) we have assumed $P_{Ar} = P$. Typically it was found that a 3rd order polynomial adequately fitted the data. We are only interested in the first two coefficients $A_0$ and $A_1$ given by

$$A_0 = \alpha/\zeta \quad (21)$$

and

$$A_1 = \frac{a_{Ar}}{\zeta} - \frac{\eta a}{\zeta^2} \tag{22}$$

We have abbreviated $\zeta = (\gamma + \xi_{F_2} P_{F_2} + \xi_{Xe} P_{Xe})$ and $\eta = \xi_{Ar} + \delta_{Xe} P_{Xe}$). By using Brashears, Setser and DesMarteau's results[12] for $\xi_{F_2}$ and $\xi_{Xe}$ and assuming $\eta a / \zeta a_{Ar} \ll 1$ (this assumption, which allows neglecting the second term in Eq. (22) was verified aposteriori), $a$ and $a_{Ar}$ were then calculated for each run from (3) and (22).

We now define a quantity $L(P_{Ar})$ given by

$$L(P_{Ar}) = \frac{a + a_{Ar} P_{Ar}}{S} - \zeta \tag{23}$$

From Eq. (19)

$$L(P_{Ar}) = \eta P_{Ar} + \delta_{Ar} P_{Ar}^2 \tag{24}$$

By at least squares fit, of a quadratic in $P_{Ar}$, to the experimental values of $L(P_{Ar})$, $\eta$ and $\delta_{Ar}$ were evaluated for each run. By plotting $\eta$ vs $P_{Xe}$, we obtained values for $\xi_{Ar}$ and $\delta_{Xe}$.

D. RESULTS AND CONCLUSIONS

Figure 7 shows the temporal variation of the e-beam current and $XeF^*$ fluorescence as detected by the photodiode. Figure 8 shows a typical curve of the measured photodiode signal as a function of Ar pressure for the special case of 22.8 torr Xe and 7.6 torr $F_2$. Figure 9 shows a reduction of the data shown in Figure 8 to the form given by Eq. (24). Also shown is at least squares fit to the reduced data to obtain the value of $\eta \delta_{Ar}$. Finally in Figure 8, Eq. (19) is plotted with the derived values of $a_{Ar}$, $\xi_{Ar}$, etc.

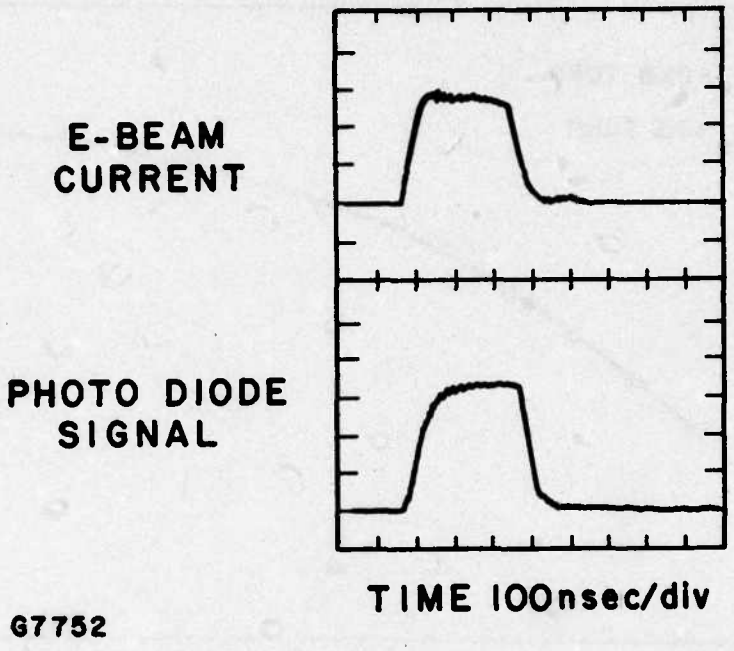


Figure 7 Typical Experimental Data. The top trace is the e-beam current and the lower trace is the photodiode response.

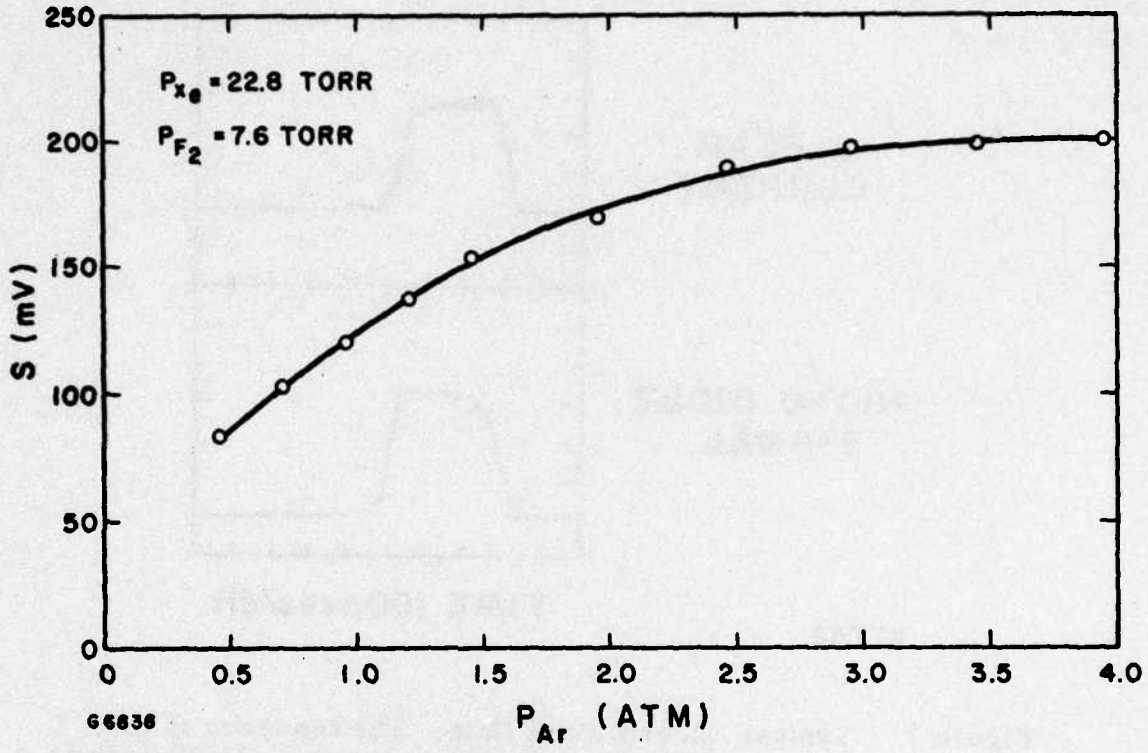


Figure 8 The Open Circles are the Experimental Measurements of the $XeF^*$ Radiation Detected by a Photodiode. Each experimental value shown above is the average of many data points. The signal was through a 5 nm bandpass filter centered at 352 nm. The curve is a plot of Eq. (19).

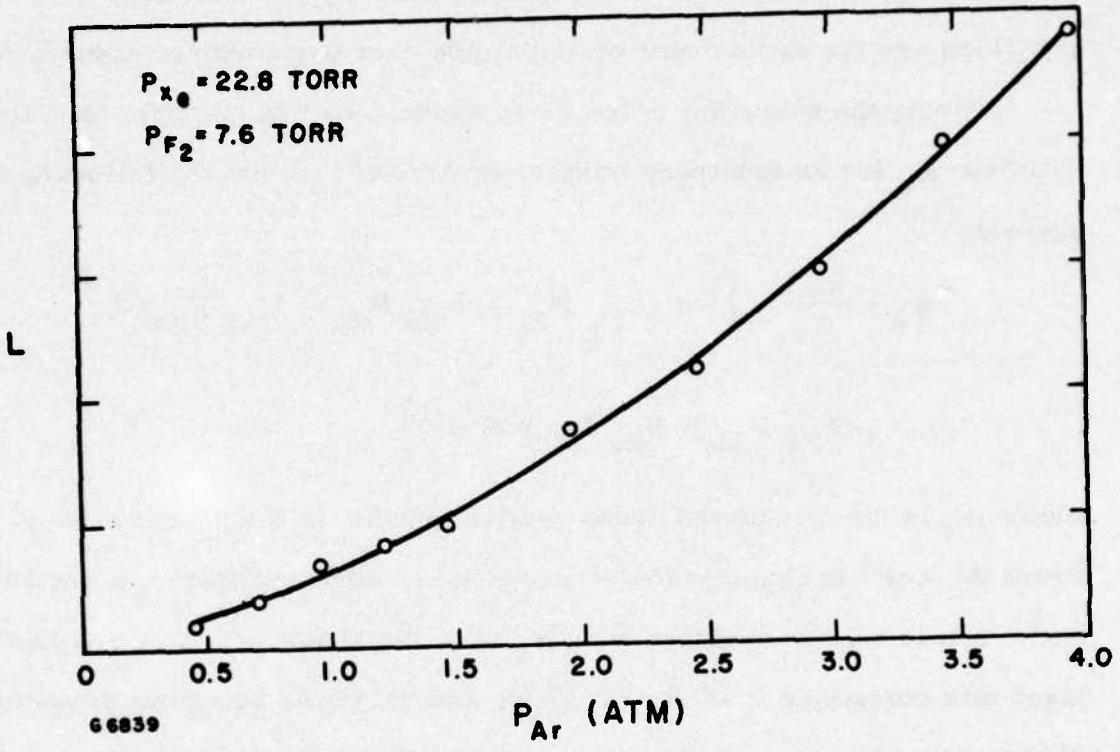


Figure 9 The Open Circles are the Data Shown in Figure 8 Reduced to Eq. (23). The curve is a least squares fit to a quadratic in $P_{Ar}$.

From these derived values we have also determined that for this case $(\eta a)/(\xi a_{Ar}) \approx 10^{-2}$. The value of $\delta_{Ar}$ was obtained by averaging the results of the many different runs performed. The large possible errors in the measured rates is because the loss of $XeF^*$ by two and three body quenching are the same order of magnitude over our range of experiments.

Using the quenching rates given above, one can compute the saturation flux $\phi_s$ for an arbitrary mixture of $Ar/Xe/F_2$ from the following expression[13]

$$\phi_s = \frac{h\nu\gamma}{\sigma_s} \left[1 + (\xi_{F_2} P_{F_2} + \xi_{Xe} P_{Xe} + \xi_{Ar} P_{Ar}) \gamma^{-1} + (\delta_{Xe} P_{Xe} + \delta_{Ar} P_{Ar}) P \gamma^{-1}\right] \quad (25)$$

where $\sigma_s$ is the stimulated cross section and $h\nu$ is the photon energy. From the $XeF^*$ spontaneous spectra we have estimated that $\sigma_s \approx 4 \times 10^{-16}$ $cm^2$. Hence we can evaluate $h\nu\gamma/\sigma_s$ to 0.084 $MW/cm^2$. For a typical laser mix containing 0.1% $F_2$, 0.5% Xe and 99.4% Ar at a total pressure of two atmospheres, one obtains $\phi_s \sigma$ 0.13 $MW/cm^2$. It should be noted that this saturation flux is correct in the limit that the ground state population is negligible.

In most e-beam pumped $XeF^*$ laser experiments performed to date $NF_3$ has been used as the halogen bearing compound.[14,15,16] Brasheans

---

(13) Physically $\phi_s$ is the flux that reduced the gain to half the small signal gain.

(14) L. F. Champagne, J.G. Eden, N.W. Harris and S.K. Searles, 3rd Summer Colloquium on Electronic Transition Lasers, Sept. 7-10 (1976).

(15) E.R. Ault, R.S. Bradford, Jr. and M.L. Bhaumik, Appl. Phys. Lett. 27, 413 (1975).

(16) C.A. Brau and J.J. Ewing (unpublished).

et al.[12] have determined that the $NF_3$ quenching rate of $XeF^*$ is 16-17 times slower than $F_2$. So $\phi_s$ for a mix containing $NF_3$ will be somewhat smaller than the value calculated above. Further, $NF_3$ does not absorb at 350 nm.[17] In spite of these two considerations, the highest laser efficiencies obtained in $XeF^*$ have been about 5%.[16,17] The maximum expected efficiency is 17%.[18] A possible explanation for the lower efficiencies obtained experimentally is photoabsorption due to charged particles (for example $F^-$)[19] and excited states (for example $Xe^*$, $Ar^*$, etc.).[20]

---

(17) S.R. LaPaglia and A.B.F. Duncan, J. Chem. Phys. 34, 1003 (1961).

(18) The metastable production efficiency in e-beam pumped Ar is about 55%. (See for example L.R. Peterson and J.E. Allen, J. Chem. Phys. 56, 6068 (1972).) The maximum $XeF^*$ efficiency quoted is just the product of the quantum efficiency and the $Ar^*$ production efficiency.

(19) A. Mandl, Phys. Rev. A3, 251 (1971).

(20) H. Hyman, AERL, private communication.

## REFERENCES


1. C.A. Brau and J.J. Ewing, Appl. Phys. Lett. 27, 435 (1975).

2. R. Burnham, D. Harris and N. Djeu, Appl. Phys. Lett. 28, 86 (1976).

3. D.C. Sutton, S.N. Suchard, O.L. Gibb and C.P. Wang, Appl. Phys. Lett. 28, 522 (1976).

4. J.A. Mangano, J.H. Jacob and J.B. Dodge, Appl. Phys. Lett., October 1, 1976.

5. J.H. Jacob and J.A. Mangano, Appl. Phys. Lett. 28, 724 (1976).

6. L.G. Piper, J.E. Velazco and D.W. Setser, J. Chem. Phys. 59, 3323 (1973).

7. M. Bourene, O. Dutnuit and J. LeCalve, J. Chem. Phys. 63, 1668 (1975).

8. J.E. Velazco, J.H. Kolts and D.W. Setser, J. Chem. Phys. 65, 3468 (1976).

9. W.W. Rigrod, J. Appl. Phys. 36, 2487 (1965).

10. A. Hawryluk, J.A. Mangano and J.H. Jacob, 3rd Summer Colloquium on Electronic Transition Lasers, Sept. 7-10 (1976). D.C. Lorents, R.M. Hill, D.L. Huestis, M.V. McCusker and N.H. Nakano, ibid.

11. G.J. Eden and S.K. Searles, 3rd Summer Colloquium on Electronic Transition Lasers, Sept. 7-10 (1976).

12. H.C. Brashears, Jr., D.W. Setser and D. DesMarteau (unpublished). These experiments were performed by photodissociating $XeF_2$ in a cell capable of going to one atmosphere.

13. Physically $\phi_s$ is the flux that reduces the gain to half the small signal gain.

14. L.F. Champagne, J.G. Eden, N.W. Harris and S.K. Searles, 3rd Summer Colloquium on Electronic Transition Lasers, Sept. 7-10 (1976).

15. E.R. Ault, R.S. Bradford, Jr. and M.L. Bhaumik, Appl. Phys. Lett. 27, 413 (1975).

16. C.A. Brau and J.J. Ewing (unpublished).

17. S.R. LaPaglia and A.B.F. Duncan, J. Chem. Phys. 34, 1003 (1961).

18. The metastable production efficiency in e-beam pumped Ar is about 55%. (See for example L.R. Peterson and J.E. Allen, J. Chem. Phys. 56, 6068 (1972).) The maximum XeF* efficiency quoted is just the product of the quantum efficiency and the $Ar^*$ production efficiency.

19. A. Mandl, Phys. Rev. A3, 251 (1971).

20. H. Hyman, AERL, private comminication.

# APPENDIX A

# ELECTRON-BEAM-CONTROLLED DISCHARGE PUMPING OF THE XeF LASER

## APPENDIX A

## ELECTRON-BEAM-CONTROLLED DISCHARGE PUMPING OF THE XeF LASER

In the last year there has been considerable interest in rare-gas monohalide lasers. These lasers were first pumped by high-energy e-beams.[1-4] The first discharge-pumped rare-gas monohalide laser was $KrF^*$.[5] This was achieved with an e-beam-controlled discharge. Subsequently, lasing action has been obtained in both $XeF^*$ and $KrF^*$ by fast discharge techniques.[6, 7] In this letter we wish to report e-beam-controlled discharge pumping of $XeF^*$.

The KrF laser discharge has been investigated in some detail[8, 9] and we expect the physics of the XeF discharge to be very similar. Electron impact excitation and ionization of the rare-gas metastables are important in determining the efficiency and stability of the XeF laser discharge.

---


(1) S.K. Searles and C.A. Hart, Appl. Phys. Lett, 27, 243 (1975).

(2) C.A. Brau and J.J. Ewing, Appl. Phys. Lett. 27, 435 (1975).

(3) J.J. Ewing and C.A. Brau, Appl. Phys. Lett. 27, 350 (1975).

(4) E.R. Ault, R.S. Bradford, and M.L. Bhaumik, Appl. Phys. Lett. 27, 412 (1975).

(5) J.A. Mangano and J.H. Jacob, Appl. Phys. Lett. 27, 495 (1975).

(6) R. Burnham, D. Harris, and N. Djeu, Appl. Phys. Lett. 28, 86 (1976).

(7) D.G. Sutton, S.H. Suchard, D.L. Gibb, and C.P. Wang, Appl. Phys. Lett. 28, 522 (1976).

(8) J.D. Daugherty, J.A. Mangano, and J.H. Jacob, Appl. Phys. Lett. 28, 581 (1976).

(9) J.H. Jacob and J.A. Mangano, Appl. Phys. Lett. 28, 724 (1976).

However, it should be possible to have stable discharges in the XeF laser mixtures if we ensure that the $F_2$ or $NF_3$ attachment rate is equal to or greater than twice the metastable ionization rate.[8]

The experimental apparatus used for the laser experiments has been described previously.[5] The cold cathode gun was modified to provide a high-energy electron current density of 12 $A/cm^2$. Even with these current densities, no lasing action was observed when the capacitor was uncharged (e-beam only). The best lasing results were obtained with mixtures of 99.5% Ar, 0.4% Xe, and 0.1% $NF_3$ at a total pressure of 4 atm. Figure A-1 shows the temporal variation of the e-beam current, discharge voltage and current, and photodiode signal. The laser pulse energy of 10 mJ was measured by a Scientech calorimeter (model 360203) and by a calibrated photodiode. The mirrors used under these conditions were a 30% output coupler and a max (> 99%) reflector. Both mirrors had a radius of curvature of 1 m and were placed 100 cm apart. The discharge was unstable and arced about 80 nsec after the capacitor voltage was switched across the anode and cathode. The mean discharge current was 75 $A/cm^2$ and the mean electric field was 11 kV/cm. The discharge energy into the mixture was about 4.9 J. The energy deposited by the high-energy e-beam was about 2.1 J. Hence the laser efficiency was only 0.3%. In Figure A-2 the top two traces show the spontaneous emission spectra when the discharge capacitor is uncharged (e-beam only) and when the capacitor is charged to 30 kV. The difference between the two spectra is the result of the discharge arcing. The bottom trace shows the XeF laser spectrum. Lasing action occurs on two lines which have been identified as radiation from primarily 0-3 and 1-4 bands.[10] The laser and spontaneous emission are red degraded, indicative

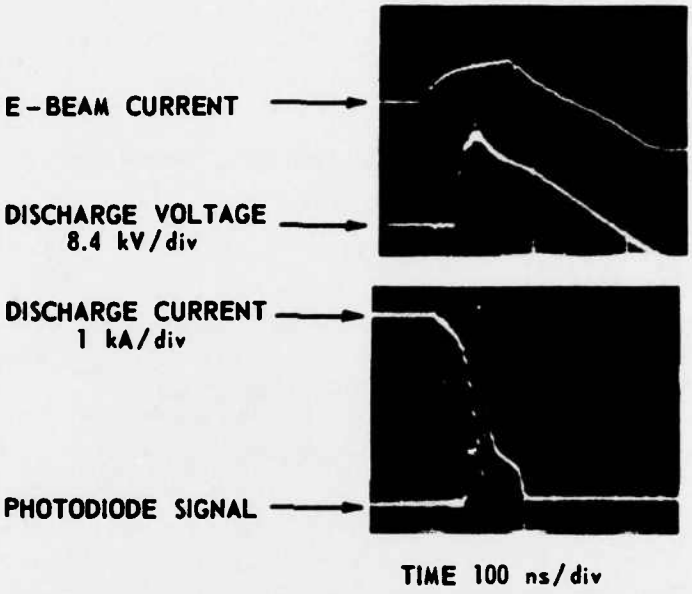


Figure A-1 Oscillograms Showing Temporal Variation of E-Beam Current, Discharge Voltage, Discharge Current, and Laser Pulse

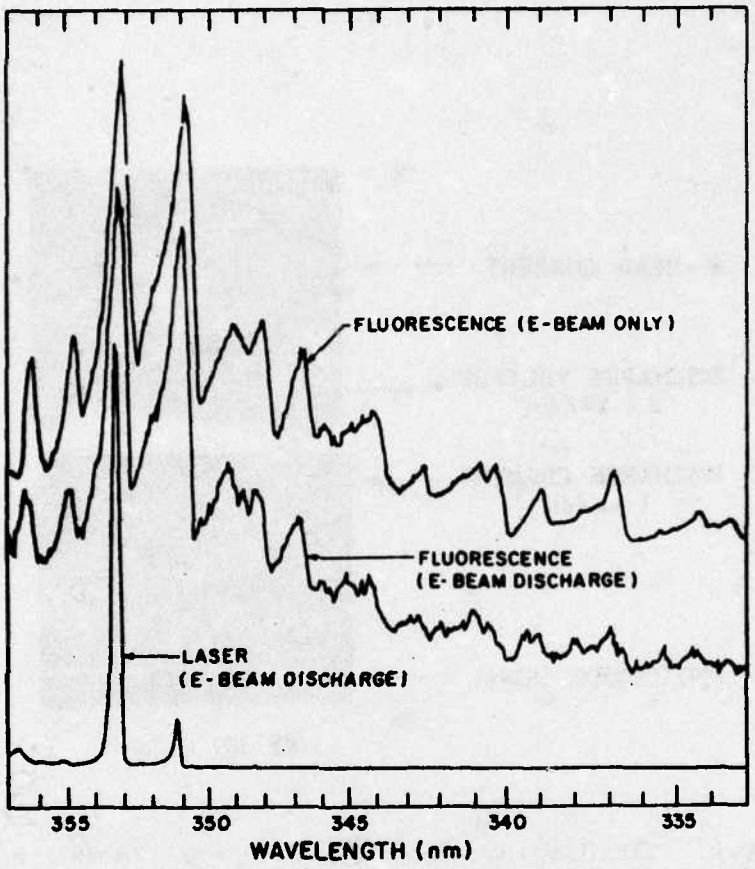


Figure A-2 Spontaneous Emission and Laser Spectra of XeF

of the fact that the internuclear separation of the upper level is larger than the lower level.

Before discussing the reason for the observed efficiency, we will attempt to establish the kinetic chain that results in $XeF^*$. By discharge pumping the secondary electrons gain enough energy in the applied electric field to excite the rare-gas metastables. We have verified, using the AERL Boltzmann code, that for laser mixtures containing 99.5% Ar and 0.4% Xe, most of the discharge energy goes into producing the argon metastables by the following reaction

$$e_d + Ar \rightarrow Ar^* + e_d. \qquad (A\text{-}1)$$

There are three prinicpal reactions by which the argon metstables are lost

$$Ar^* + Xe \rightarrow Xe^* + Ar, \qquad (A\text{-}2)$$

$$Ar^* + 2Ar \rightarrow Ar_2^* + Ar, \qquad (A\text{-}3)$$

$$Ar^* + NF_3 \rightarrow ArF^* + NF_2. \qquad (A\text{-}4)$$

The rate constant for reaction (A-2) has been measured to be $1.8 \times 10^{-10}$ and $3 \times 10^{-10}$ $cm^3/sec$ for Ar ($^3P_2$) and Ar ($^3P_0$), respectively.[11] Reaction (A-3) has a three-body rate constant of $1.7 \times 10^{-32}$ $cm^6/sec$ for Ar ($^3P_1$), $0.9 \times 10^{-32}$ $cm^6/sec$ for Ar ($^1P_1$), and $1.6 \times 10^{-32}$ $cm^6/sec$ for Ar ($^3P_2$).[12] Assuming a gas kinetic mixing rate of these states by electrons, the loss rates of $Ar^*$ by reactions (A-2) and (A-3) will be only marginally

---

(10) Joel Tellingheusen, G.C. Tisone, J.M. Hoffman, and A.K. Hays (unpublished).

(11) L.G. Piper, J.E. Velazco, and D.W. Setser, J. Chem. Phys. 59, 3323 (1973).

(12) M Bourene, O. Dutuit, and J. LeCalve, J. Chem. Phys. 63, 1668 (1975).

affected. So we will assume a mean rate of $2 \times 10^{-10}$ $cm^3/sec$ for reaction (A-2) and $10^{-32}$ $cm^3/sec$ for reaction (A-3). The argon metastables react with $NF_3$ to form $ArF^*$ with a rate constant of $1.4 \times 10^{-10}$ $cm^3/sec$.[13] The branching ratio for this reaction is yet to be determined. Extrapolating from reactions of $Xe^*$ and $Kr^*$ with $NF_3$[12] one might conclude that reaction (A-3) has a branching ratio of about 0.5. At a mixture pressure of 4 atm with 0.4% Xe and 0.1% $NF_3$, the rates for reactions (A-2) - (A-4) are $8 \times 10^7$, $2.5 \times 10^7$, and $1.4 \times 10^7$ $cm^3/sec$. So about 15% of the $Ar^*$ is channeled into $ArF^*$. It is possible that some of the energy in $ArF^*$ will produce $XeF^*$ by the following reaction:

$$ArF^* + Xe \rightarrow XeF^* + Ar. \qquad \text{(A-5)}$$

The remainder of the energy is presumably radiated on the $ArF^*$ bands. Reaction (A-5) will have to proceed at a gas kinetic rate if 50% of the $ArF^*$ is to be channeled into $XeF^*$.

The argon excimers will be deactivated at least as rapidly[14] by Xe to form $Xe^*$, which means that 70-80% of the $Ar_2^*$ will end up as $Xe^*$. The remainder of the $Ar_2^*$ will be radiated. So we can conclude that the argon metastables transfer their energy to the xenon metastables with a 75% efficiency. The $Xe^*$ thus formed will react with the $NF_3$ to form $XeF^*$ with a unit branching ratio.[12] The rate constant for this reaction is $9 \times 10^{-11}$ $cm^3/sec$. Hence the $Xe^*$ lifetime is 100 nsec. This perhaps explains why the laser power drops rapidly after the discharge arcs, but lasing continues at ever decreasing power for another 100 nsec. (See Figure A-1.) In the case of $KrF^*$ and $Br_2^*$, the laser action terminated

---

(13) J.E. Velazco, J.H. Kolts, and D.W. Setser (unpublished).

(14) According to D.W. Setser a rate constant in excess of the gas kinetic rate is not likely.

much more rapidly.[5,15] This occurs because both $F_2$ and $Br_2$ quench the rare-gas metastables much more rapidly than $NF_3$.[12] Perhaps half of the $Ar^*$ that does not form $Xe^*$ will result in $XeF^*$ production. So the effective branching ratio for producing $XeF^*$ from $Ar^*$ is between 0.75 and 0.9.

When the $NF_3$ is replaced by $F_2$, 50% of the argon metastables are channeled into $ArF^*$. This is because the reaction that is equivalent to (A-4), i.e.,

$$Ar^* + F_2 \rightarrow ArF^* + F, \qquad \text{(A-6)}$$

proceeds at a 7-8 times faster rate[12] and probably has a higher branching ratio. If the lifetime of $ArF^*$ is the same as $KrF^*$ ($\approx$10 nsec), then even if the rate for reaction (A-5) were gas kinetic, only about 50% of the energy in $ArF^*$ would result in $XeF^*$. So the effective branching ratio with $F_2$ is 0.5-0.75. With $F_2$ mixtures we have observed that the fluorescence is smaller by about a factor of 5. This reduced fluorescence cannot be explained by the above kinetics. It is possible that $F_2$ deactivates $XeF^*$ with a rate constant of $5 \times 10^{-10}$ $cm^3/sec$. If the radiative lifetime of $XeF^*$ is in fact 50 nsec,[13,16] and assuming that the deactivation of $XeF^*$ is negligible, the relative decreased fluorescence can then be understood.

A laser efficiency of 0.3% was obtained with 0.1% $NF_3$, 0.4% Xe, 99.5% Ar mix at 4 atm. From the fluorescence enhancement when the discharge was applied (over that achieved with the e-beam alone) we estimate the efficiency of producing argon metastables to be about 25%. Using the estimated branching ratio of 0.8 and a quantum efficiency of 35%, we estimate that the production efficiency for $XeF^*$ is 7% which is still about

(15) J.J. Ewing, J.H. Jacob, J.A. Mangano, and H. Brown, Appl. Phys. Lett. 28, 656 (1976).

(16) C.A. Brau and J.J. Ewing (unpublished).

20 times larger than the observed laser efficiency. There are two possible reasons for the difference between the production efficiency and laser efficiency. First the cavity flux could have been a factor of 10 or so smaller than the saturation flux $\phi_s$, which can be expressed as

$$\phi_s = (h\nu/\sigma_s\tau_r)(1 + \tau_r/\tau_q),$$

where $h\nu$ is the photon energy, $\sigma_s$ is the stimulated emission cross section, and $\tau_r$ and $\tau_q$ are the radiative lifetime and inverse quenching rate of $XeF^*$, respectively. The cavity flux is estimated to be about $3 \times 10^5$ $W/cm^2$. To explain the observed laser efficiency, $\phi_s$ would have to be about $3 \times 10^5$ $W/cm^2$. From this we can infer that $\tau_q$ has to be of order 5 nsec. Such a rapid quenching rate would be possible if xenon quenched $XeF^*$ with a rate constant of $5 \times 10^{-10}$ $cm^3/sec$.[17] Another possibility is that the electrons quench $XeF^*$ with a rate constant of $3 \times 10^{-8}$ $cm^3/sec$ which implies a cross section of about $3 \times 10^{-16}$ $cm^2$.

A second possible explanation for the difference between production efficiency and laser efficiency is excited state absorption. Under conditions of the experiment we estimate the rare-gas metastable density to be about $5 \times 10^{15}/cm^3$. The photoabsorption cross section would then have to be about $1.5 \times 10^{-17}$ $cm^2$ to explain the observed efficiency. However, such a cross section for photoionization of the metastables is unlikely.[18] Also, since high ($\approx$6%) efficiencies were obtained in the $XeF^*$ laser with e-beam pumping,[19] it is unlikely that excited states can have such a high photoabsorption cross section.

---

(17) It is also a possibility that $NF_3$ quenching is important. This implies a reaction rate of $2 \times 10^{-9}$ $cm^3/sec$.

(18) H. Hyman (private communication).

(19) C.A. Brau and J.J. Ewing (unpublished).

In conclusion, the most likely mechanism responsible for the observed efficiency in $XeF^*$ is quenching of $XeF^*$ by heavy bodies such as Xe or Ar. If so, the efficiency can be increased by increasing the laser cavity flux.

The authors wish to thank J.D. Daugherty and D.W. Setser for many useful discussions during the course of this work.

# APPENDIX A

## REFERENCES


1. S.K. Searles and C.A. Hart, Appl. Phys. Lett. 27, 243 (1975).
2. C.A. Brau and J.J. Ewing, Appl. Phys. Lett. 27, 435 (1975).
3. J.J. Ewing and C.A. Brau, Appl. Phys. Lett. 27, 350 (1975).
4. E.R. Ault, R.S. Bradford, and M.L. Bhaumik, Appl. Phys. Lett. 27, 412 (1975).
5. J.A. Mangano and J.H. Jacob, Appl. Phys. Lett. 27, 495 (1975).
6. R. Burnham, D. Harris, and N. Djeu, Appl. Phys. Lett. 28, 86 (1976).
7. D.G. Sutton, S.H. Suchard, D.L. Gibb, and C.P. Wang, Appl. Phys. Lett. 28, 522 (1976).
8. J.D. Daugherty, J.A. Mangano, and J.H. Jacob, Appl. Phys. Lett. 28, 581 (1976).
9. J.H. Jacob and J A. Mangano, Appl. Phys. Lett. 28, 724 (1976).
10. Joel Tellingheusen, G.C. Tisone, J.M. Hoffman, and A.K. Hays (unpublished).
11. L.G. Piper, J.E. Velazco, and D.W. Setser, J. Chem. Phys. 59, 3323 (1973).
12. M. Bourene, O. Dutuit, and J. LeCalve, J. Chem. Phys. 63, 1668 (1975).
13. J.E. Velazco, J.H. Kolts, and D.W. Setser (unpublished).
14. According to D.W. Setser a rate constant in excess of the gas kinetic rate is not likely.
15. J.J. Ewing, J.H. Jacob, J.A. Mangano, and H. Brown, Appl. Phys Lett. 28, 656 (1976).
16. C.A. Brau and J.J. Ewing (unpublished).
17. It is also a possibility that $NF_3$ quenching is important. This implies a reaction rate of $2 \times 10^{-9}$ $cm^3/sec$.
18. H. Hyman (private communication).
19. C.A. Brau and J.J. Ewing (unpublished).

## DISTRIBUTION LIST

Office of Naval Research, Department of the Navy, Arlington, VA 22217 - Attn: Physics Program (3 copies)

Naval Research Laboratory, Department of the Navy, Washington, D.C. 20375 - Attn: Technical Library (1 copy)

Office of the Director of Defense, Research and Engineering, Information Office Library Branch, The Pentagon, Washington, D.C. 20301 (1 copy)

U.S. Army Research Office, Box CM, Duke Station, Durham, N.C. 27706 (1 copy)

Defense Documentation Center, Cameron Station, Alexandria, VA 22314 (12 copies)

Defender Information Analysis Center, Battelle Memorial Institute, 505 King Avenue, Columbus, OH 43201 (1 copy)

Commanding Officer, Office of Naval Research Branch Office, 536 South Clark Street, Chicago, IL 60615 (1 copy)

New York Area Office, Office of Naval Research, 715 Broadway (5th Floor), New York, NY 10003 - Attn: Dr. Irving Rowe (1 copy)

San Francisco Area Office, Office of Naval Research, 760 Market Street, Room 447, San Francisco, CA 94102 (1 copy)

Air Force Office of Scientific Research, Department of the Air Force, Washington, D.C. 22209 (1 copy)

Office of Naval Research Branch Office, 1030 East Green Street, Pasadena, CA 91106 - Attn: Dr. Robert Behringer (1 copy)

Code 102 IP (ONRL), Office of Naval Research, 800 N. Quincy Street, Arlington, VA 22217 (6 copies)

Defense Advanced Research Projects Agency, 1400 Wilson Blvd., Arlington, VA 22209 - Attn: Strategic Technology Office (1 copy)

Office Director of Defense, Research & Engineering, The Pentagon, Washington, D.C. 20301 - Attn: Assistant Director (Space and Advanced Systems) (1 copy)

Office of the Assistant Secretary of Defense, System Analysis (Strategic Programs), Washington, D.C. 20301 - Attn: Mr. Gerald R. McNichols (1 copy)

U.S. Arms Control and Disarmament Agency, Dept. of State Bldg., Rm. 4931, Washington, D.C. 20451 - Attn: Dr. Charles Heskin (1 copy)

Energy Research Development Agency, Division of Military Applications, Washington, D.C. 20545 (1 copy)

National Aeronautics and Space Administration, Lewis Research Center, Cleveland, OH 44135 - Attn: Dr. John W. Dunning, Jr. (1 copy)
(Aerospace Res. Engineer)

National Aeronautics & Space Administration, Code RR, FOB 10B, 600 Independence Ave., SW, Washington, D.C. 20546 (1 copy)

National Aeronautics and Space Administration, Ames Research Center, Moffett Field, CA 94035 - Attn: Dr. Kenneth W. Billman (1 copy)

Department of the Army, Office of the Chief of RD&A, Washington, D.C. 20310 - Attn: DARD-DD (1 copy)
DAMA-WSM-T (1 copy)

Department of the Army, Office of the Deputy Chief of Staff for Operations & Plans, Washington, D.C. 20310 - Attn: DAMO-RQD - (1 copy)

Ballistic Missile Defense Program Office (BMDPO), The Commonwealth Building, 1300 Wilson Blvd., Arlington, VA 22209 - Attn: Mr. Albert J. Bast, Jr. (1 copy)

U.S. Army Missile Command, Research & Development Division, Redstone Arsenal, AL 35809 - Attn: Army High Energy Laser Programs (2 copies)

Commander, Rock Island Arsenal, Rock Island, IL 61201, Attn: SARRI-LR, Mr. J.W. McGarvey (1 copy)

Commanding Officer, U.S. Army Mobility Equipment R&D Center, Ft. Belvoir, VA 22060 - Attn: SMEFB-MW (1 copy)

Commander, U.S. Army Armament Command, Rock Island, IL 61201 - Attn: AMSAR-RDT (1 copy)

Director, Ballistic Missile Defense Advanced Technology Center, P.O. Box 1500, Huntsville AL 35807 - Attn: ATC-O (1 copy)
ACT-T (1 copy)

Commander, U.S. Army Material Command, Alexandria, VA 22304 - Attn: Mr. Paul Chernoff (AMCRD-T) (1 copy)

Commanding General, U.S. Army Munitions Command, Dover, NH 17801 - Attn: Mr. Gilbert F. Chesnov (AMSMU-R) (1 copy)

Director, U.S. Army Ballistics Res. Lab, Aberdeen Proving Ground, MD 21005 - Attn: Dr. Robert Eichenberger (1 copy)

Commandant, U.S. Army, Air Defense School, Ft. Bliss, TX 79916 - Attn: Air Defense Agency (1 copy)
ATSA-CTD-MS (1 copy)

Commanding General, U.S. Army Combat Dev. Command, Ft. Belvoir, VA 22060 - Attn: Director of Material, Missile Div. (1 copy)

Commander, U.S. Army Training & Doctrine Command, Ft. Monroe, VA 23651 - Attn: ATCD-CF (1 copy)

Commander, U.S. Army Frankford Arsenal, Philadelphia, PA 19137 - Attn: Mr. M. Elnick SARFA-FCD Bldg. 201-3 (1 copy)

Commander, U.S. Army Electronics Command, Ft. Monmouth, NJ 07703 - Attn: AMSEL-CT-L, Dr. R.G. Bueer (1 copy)

Commander, U.S. Army Combined Arms Combat Developments Activity, Ft. Leavenworth, KS 66027 (1 copy)

National Security Agency, Ft. Geo. G. Meade, MD 20755 - Attn: R.C. Foss A763 (1 copy)

Deputy Commandant for Combat & Training Developments, U.S. Army Ordnance Center and School, Aberdeen Proving Ground, MD 21005
Attn: ATSL-CTD-MS-R (1 copy)

Commanding Officer, USACDC CBR Agency, Ft. McClellan, AL 36201 - Attn: CDCCBR-MR (Mr. F.D. Poer) (1 copy)

DISTRIBUTION LIST (Continued)

Department of the Navy, Office of the Chief of Naval Operations, The Pentagon 5C739, Washington, D.C. 20350 - Attn: (OP 982F3) (1 copy)

Office of Naval Research Branch Office, 495 Summer Street, Boston, MA 02210 - Attn: Dr. Fred Quelle (1 copy)

Department of the Navy, Deputy Chief of Navy Material (Dev.), Washington, D.C. 20360 - Attn: Mr. R. Gaylord (MAT 032B) (1 copy)

Naval Missile Center, Point Mugu, CA 93042 - Attn: Gary Gibbs (Code 5352) (1 copy)

Naval Research Laboratory, Washington, D.C. 20375 - Attn: (Code 5503-EOTPO) (1 copy)
Dr. P. Livingston - Code 5560 (1 copy)
Dr. A. L. Schindler - Code 6000 (1 copy)
Dr. H. Shocker - Code 5504 (1 copy)
Mr. D.J. McLaughlin - Code 5560 (1 copy)
Dr. John L. Walsh - Code 5503 (1 copy)

High Energy Laser Project Office, Department of the Navy, Naval Sea Systems Command, Washington, D.C. 20360 - Attn: Capt. A. Skolnick, USN (PM 22) (1 copy)

Superintendent, Naval Postgraduate School, Monterey, CA 93940 - Attn: Library (Code 2124) (1 copy)

Navy Radiation Technology, Air Force Weapons Lab (NLO), Kirtland AFB, NM 87117 (1 copy)

Naval Surface Weapons Center, White Oak, Silver Spring, MD 20910 - Attn: Dr. Leon H. Schindel (Code 310) (1 copy)
Dr. E. Leroy Harris (Code 313) (1 copy)
Mr. K. Eckenhaus (Code 034) (1 copy)
Mr. J. Wise (Code 047) (1 copy)
Technical Library (1 copy)

U.S. Naval Weapons Center, China Lake, CA 93555 - Attn: Technical Library (1 copy)

HQ USAF (AF/RDPS), The Pentagon, Washington, D.C. 20330 - Attn: Lt. Col. A.J. Chiota (1 copy)

HQ AFSC/XRLW, Andrews AFB, Washington, D.C. 20331 - Attn: Maj. J.M. Wilson (1 copy)

HQ AFSC (DLCAW), Andrews AFB, Washington, D.C. 20331 - Attn: Maj. H. Axelrod (1 copy)

Air Force Weapons Laboratory, Kirtland AFB, NM 87117 - Attn: LR (1 copy)
AL (1 copy)

HQ SAMSO (XRTD), P.O. Box 92960, Worldway Postal Center, Los Angeles, CA 90009 - Attn: Lt. Dorice DeMelo (XRTD) (1 copy)

AF Avionics Lab (TEO), Wright Patterson AFB, OH 45433 - Attn: Mr. K. Hutchinson (1 copy)

Dept. of the Air Force, Air Force Materiel Lab. (AFSC), Wright Patterson AFB, OH 45433 - Attn: Maj. Paul Elder (LPS) (1 copy)
Laser Window Group

HQ Aeronautical Systems Div., Wright Patterson AFB, OH 45433 - Attn: XRF - Mr. Clifford Fawcett (1 copy)

Rome Air Development Command, Griffiss AFB, Rome, NY 13440 - Attn: Mr. R. Urtz (OCSE) (1 copy)

HQ Electronics Systems Div. (ESL), L.G. Hanscom Field, Bedford, MA 01730 - Attn: Mr. Alfred E. Anderson (XRT) (1 copy)
Technical Library (1 copy)

Air Force Rocket Propulsion Lab., Edwards AFB, CA 93523 - Attn: B.R. Bornhorst, (LKCG) (1 copy)

Air Force Aero Propulsion Lab., Wright Patterson AFB, OH 45433 - Attn: Col. Walter Moe (CC) (1 copy)

Dept. of the Air Force, Foreign Technology Division, Wright Patterson AFB, OH 45433 - Attn: PDTN (1 copy)

Commandant of the Marine Corps, Scientific Advisor (Code RD-1), Washington, D.C. 20380 (1 copy)

Aerospace Research Labs., (AP), Wright Patterson AFB, OH 45433 - Attn: Lt. Col. Max Duggins (1 copy)

Defense Intelligence Agency, Washington, D.C. 20301 - Attn: Mr. Seymour Berler (DT1B) (1 copy)

Central Intelligence Agency, Washington, D.C. 20505 - Attn: Mr. Julian C. Nall (1 copy)

Analytic Services, Inc., 5613 Leesburg Pike, Falls Church, VA 22041 - Attn: Dr. John Davis (1 copy)

Aerospace Corp., P.O. Box 92957, Los Angeles, CA 90009 - Attn: Dr. G.P. Millburn (1 copy)

Airesearch Manuf. Co., 9851-9951 Sepulveda Blvd., Los Angeles, CA 90009 - Attn: Mr. A. Colin Stancliffe (1 copy)

Atlantic Research Corp., Shirley Highway at Edsall Road, Alexandria, VA 22314 - Attn: Mr. Robert Naismith (1 copy)

Avco Everett Research Lab., 2385 Revere Beach Parkway, Everett, MA 02149 - Attn: Dr. George Sutton (1 copy)
Dr. Jack Daugherty (1 copy)

Battelle Columbus Laboratories, 505 King Avenue, Columbus, OH 43201 - Attn: Mr. Fred Tietzel (STPIAC) (1 copy)

Bell Aerospace Co., Buffalo, NY 14240 - Attn: Dr. Wayne C. Solomon (1 copy)

Boeing Company, P.O. Box 3999, Seattle, WA 98124 - Attn: Mr. M.L. Gamble (2-, 460, MS 8C-88) (1 copy)

Electro-Optical Systems, 300 N. Halstead, Pasadena, CA 91107 - Attn: Dr. Andrew Jensen (1 copy)

ESL, Inc., 495 Java Drive, Sunnyvale, CA 94086 - Attn: Arthur Fishorn (1 copy)

DISTRIBUTION LIST (Continued)

General Electric Co., Space Division, P.O. Box 8555, Philadelphia, PA 19101 - Attn: Dr. R.R. Sigismonti (1 copy)

General Electric Co., 100 Plastics Avenue, Pittsfield, MA 01201 - Attn: Mr. D.G. Herrington (Rm. 1044) (1 copy)

General Research Corp., P.O. Box 3587, Santa Barbara, CA 93105 - Attn: Dr. R. Holbrook (1 copy)

General Research Corp., 1501 Wilson Blvd., Suite 700, Arlington, VA 22209 - Attn: Dr. Giles F. Criml (1 copy)

Hercules, Inc., Industrial System Dept., Wilmington, DE 19899 - Attn: Dr. R.S. Voris (1 copy)

Hercules, Inc., P.O. Box 210, Cumberland, MD 21502 - Attn: Dr. Ralph R. Preckel (1 copy)

Hughes Research Labs., 3011 Malibu Canyon Road, Malibu, CA 90265 - Attn: Dr. D. Forster (1 copy)

Hughes Aircraft Co., Aerospace Group - Systems Division, Canoga Park, CA 91304 - Attn: Dr. Jack A. Alcalay (1 copy)

Hughes Aircraft Co., Centinela and Teale Streets, Bldg. 6, MS E-125, Culver City, CA 90230 - Attn: Dr. William Yates (1 copy)

Institute for Defense Analyses, 400 Army-Navy Drive, Arlington, VA 22202 - Attn: Dr. Alvin Schnitzler (1 copy)

Johns Hopkins University, Applied Physics Lab., 8621 Georgia Avenue, Silver Spring, MD 20910 - Attn: Dr. Albert M. Stone (1 copy)

Lawrence Livermore Laboratory, P.O. Box 808, Livermore, CA 94550 - Attn: Dr. R.E. Kidder (1 copy)
Dr. E. Teller (1 copy)
Dr. Joe Fleck (1 copy)

Los Alamos Scientific Laboratory, P.O. Box 1663, Los Alamos, NM 87544 - Attn: Dr. Keith Boyer (1 copy)

Lulejian and Associates, Inc., Del Amo Financial Center, 21515 Hawthorne Blvd. - Suite 500, Torrance, CA 90503 (1 copy)

Lockheed Palo Alto Res. Lab., 3251 Hanover St., Palo Alto, CA 94303 - Attn: L.R. Luneford, Orgn. 52-24, Bldg. 201 (1 copy)

Mathematical Sciences Northwest, Inc., P.O. Box 1887, Bellevue, WN 98009 - Attn: Dr. Abraham Herteberg (1 copy)

Martin Marietta Corp., P.O. Box 179, Mail Station 0471, Denver, CO 80201 - Attn: Mr. Stewart Chapin (1 copy)

Massachusetts Institute of Technology, Lincoln Laboratory, P.O. Box 73, Lexington, MA 02173 - Attn: Dr. S. Edelberg (1 copy)
Dr. L.C. Marquet (1 copy)

McDonnell Douglas Astronautics Co., 5301 Bolsa Avenue, Huntington Beech, CA 92647 - Attn: Mr. P.L. Klevatt, Dept. A3-830-BBPO, M/S 9 (1 copy)

McDonnell Douglas Research Labs., Dept. 220, Box 516, St. Louis, MO 63166 - Attn: Dr. D.P. Ames (1 copy)

MITRE Corp., P.O. Box 208, Bedford, MA 01730 - Attn: Mr. A.C. Cron (1 copy)

North American Rockwell Corp., Autonetics Div., Anaheim, CA 92803 - Attn: Mr. T.T. Kumagi, C/476 Mail Code HA18 (1 copy)

Northrop Corp., 3401 West Broadway, Hawthorne, CA 90250 - Attn: Dr. Gerard Hasserjian, Laser Systems Dept. (1 copy)

Dr. Anthony N. Pirri, Physical Sciences, Inc., 18 Lakeside Office Park, Wakefield, MA 01880 (1 copy)

RAND Corp., 1700 Main Street, Santa Monica, CA 90406 - Attn: Dr. C.R. Culp/Mr. G.A. Carter (1 copy)

Raytheon Co., 28 Seyon Street, Waltham, MA 02154 - Attn: Dr. F.A. Horrigan (Res. Div.) (1 copy)

Raytheon Co., Boston Post Road, Sudbury, MA 01776 - Attn: Dr. C. Sonnenschien (Equip. Div.) (1 copy)

Raytheon Co., Bedford Labs, Missile Systems Div., Bedford, MA 01730 - Attn: Dr. H.A. Mehlhorn (1 copy)

Riverside Research Institute, 80 West End Street, New York, NY 10023 - Attn: Dr. L.H. O'Neill (1 copy)
Dr. John Bose (1 copy)
(HPEGL Library) (1 copy)

R&D Associates, Inc., P.O. Box 3580, Santa Monica, CA 90431 - Attn: Dr. R.E. LaLevier (1 copy)

Rockwell International Corporation, Rocketdyne Division, Albuquerque District Office, 3636 Menaul Blvd., NE, Suite 211, Albuquerque, NM 87110 - Attn: C.K. Kreus, Mgr. (1 copy)

SANDIA Corp., P.O. Box 5800, Albuquerque, NM 87115 - Attn: Dr. Al Nareth (1 copy)

Stanford Research Institute, Menlo Park, CA 94025 - Attn: Dr. F.T. Smith (1 copy)

Science Applications, Inc., 1911 N. Ft. Meyer Drive, Arlington, VA 22209 - Attn: L. Peckam (1 copy)

Science Applications, Inc., P.O. Box 328, Ann Arbor, MI 48103 - Attn: R.E. Maredith (1 copy)

Science Applications, Inc., 6 Preston Court, Bedford, MA 01703 - Attn: R. Greenberg (1 copy)

Science Applications, Inc., P.O. Box 2351, La Jolla, CA 92037 - Attn: Dr. John Asmus (1 copy)

Systems, Science and Software, P.O. Box 1620, La Jolla, CA 92037 - Attn: Alan F. Klein (1 copy)

Systems Consultants, Inc., 1050 31st Street, NW, Washington, D.C. 20007 - Attn: Dr. R.B. Keller (1 copy)

Thiokol Chemical Corp., WASATCH Division, P.O. Box 524, Brigham City, UT 84302 - Attn: Mr. J.E. Hansen (1 copy)

TRW Systems Group, One Space Park, Bldg. R-1, Rm. 1050, Redondo Beech, CA 90278 - Attn: Mr. Norman Campbell (1 copy)

United Technologies Research Center, 400 Main Street, East Hartford, CT 06108 - Attn: Mr. G.H. McLafferty (3 copies)

**DISTRIBUTION LIST (Continued)**

United Technologies Research Center, Pratt and Whitney Aircraft Div., Florida R&D Center, West Palm Beach, FL 33402 Attn: Dr. R.A. Schmidtke (1 copy)
Mr. Ed Pinsley (1 copy)

VARIAN Associates, EIMAC Division, 301 Industrial Way, San Carlos, CA 94070 - Attn: Mr. Jack Quine (1 copy)

Vought Systems Division, LTV Aerospace Corp., P.O. Box 5907, Dallas, TX 75222 - Attn: Mr. F.G. Simpson, MS 254142 (1 copy)

Westinghouse Electric Corp., Defense and Space Center, Balt-Wash. International Airport - Box 746, Baltimore, MD 21203 - Attn: Mr. W.F. List (1 copy)

Westinghouse Research Labs., Beulah Road, Churchill Boro, Pittsburgh, PA 15235 - Attn: Dr. E.P. Riedel (1 copy)

United Technologies Research Center, East Hartford, CT 06108 - Attn: A.J. DeMaria (1 copy)

Airborne Instruments Laboratory, Walt Whitman Road, Melville, NY 11746 - Attn: F. Pace (1 copy)

General Electric R&D Center, Schenectady, NY 12305 - Attn: Dr. Donald White (1 copy)

Cleveland State University, Cleveland, OH 44115 - Attn: Dean Jack Soules (1 copy)

EXXON Research and Engineering Co., P.O. Box 8, Linden, NJ 07036 - Attn: D. Grafstein (1 copy)

University of Maryland, Department of Physics and Astronomy, College Park, MD 20742 - Attn: D. Currie (1 copy)

Sylvania Electric Products, Inc., 100 Fergeson Drive, Mountain View, CA 94040 - Attn: L.M. Osterink (1 copy)

North American Rockwell Corp., Autonetics Division, 3370 Miraloma Avenue, Anaheim, CA 92803 - Attn: R. Gudmundsen (1 copy)

Massachusetts Institute of Technology, 77 Massachusetts Avenue, Cambridge, MA 02138 - Attn: Prof. A. Javan (1 copy)

Lockheed Missile & Space Co., Palo Alto Research Laboratories, Palo Alto, CA 94304 - Attn: Dr. R.C. Chilman (1 copy)

ILC Laboratories, Inc., 164 Commercial Street, Sunnyvale, CA 94086 - Attn: L. Noble (1 copy)

University of Texas at Dallas, P.O. Box 30365, Dallas, TX 75230 - Attn: Prof. Carl B. Collins (1 copy)

Polytechnic Institute of New York, Rt. 110, Farmingdale, NY 11735 - Attn: Dr. William T. Walter (1 copy)